

ORIGINAL RESEARCH COMMUNICATION

Temporal cross-talk between endoplasmic reticulum and mitochondria regulates oxidative stress and mediates microparticle-induced endothelial dysfunction

Zainab Safiedeen^{1,2}, Isabel Rodríguez-Gómez¹, Luisa Vergori¹, Raffaella Soleti¹, Dayannath Vaithilingam¹, Imene Douma¹, Abdelali Agouni³, Denis Leiber¹, Séverine Dubois^{1,4}, Gilles Simard^{1,4}, Kazem Zibara^{2,5}, Ramaroson Andriantsitohaina^{1,4}, and M. Carmen Martínez^{1,4}

¹INSERM U1063, Stress Oxydant et Pathologies Métaboliques, Université d'Angers; Angers, France

²ER045, Laboratory of Stem Cells, PRASE, DSST, Lebanese University, Beirut, Lebanon,

³University of Surrey, Faculty of Health and Medical Sciences, Guildford, United Kingdom

⁴Centre Hospitalo-Universitaire d'Angers, Angers, France

⁵Biology Department, Faculty of Sciences-I, Lebanese University, Beirut, Lebanon

Present address of A. Agouni: Qatar University, College of Pharmacy, Doha, Qatar.

Corresponding author: M.C. Martinez, INSERM U1063, Stress Oxydant et Pathologies Métaboliques, Institut de Biologie en Santé, 4 rue Larrey, F-

49933 Angers, France. Phone: +33 2 44 68 85 79. E-mail:
carmen.martinez@univ-angers.fr

Abbreviated title: Unfolded protein response/microvesicles

Word count: 6110

Reference numbers: 34

Greyscale illustrations: 2

Color illustrations: 6 (online)

Abstract

Aims: Circulating microparticles (MPs) from metabolic syndrome patients and those generated from apoptotic T-cells induce endothelial dysfunction; however, the molecular and cellular mechanism(s) underlying in the effects of MPs remain to be elucidated. *Results:* Here, we show that both types of MPs increased expression of endoplasmic reticulum (ER) stress markers XBP-1, p-eIF2alpha and CHOP and nuclear translocation of ATF6 on human aortic endothelial cells. MPs decreased *in vitro* nitric oxide release by human aortic endothelial cells, whereas *in vivo* MP injection into mice impaired the endothelium-dependent relaxation induced by acetylcholine. These effects were prevented when ER stress was inhibited suggesting that ER stress is implicated in the endothelial effects induced by MPs. MPs affected mitochondrial function and evoked sequential increase of cytosolic and mitochondrial reactive oxygen species (ROS). Pharmacological inhibition of ER stress and silencing of neutral sphingomyelinase with siRNA abrogated all MP-mediated effects. Neutralization of Fas-Ligand carried by MPs abolished effects induced by both MP types, whereas neutralization of low density lipoprotein-receptor on endothelial cells prevented T-lymphocyte MP-mediated effects. *Innovation and Conclusion:* Collectively, endothelial dysfunction triggered by MPs involves temporal cross-talk between ER and mitochondria with respect to spatial regulation of ROS via the neutral sphingomyelinase and interaction of MPs with Fas and/or low density lipoprotein-receptor. These

results provide a novel molecular insight into the manner MPs mediate vascular dysfunction and allow identification of potential therapeutic targets to treat vascular complications associated with metabolic syndrome.

Introduction

Metabolic syndrome defines a cluster of interrelated risk factors for cardiovascular disease and diabetes. These factors include metabolic abnormalities such as hyperglycemia, elevated triglyceride levels, low high-density lipoprotein cholesterol levels, high blood pressure and obesity, mainly central adiposity. Endothelial dysfunction participates actively in the development of cardiovascular diseases associated with metabolic syndrome (17). Among biological markers of endothelium injury, microparticles (MPs) have been involved in the pathogenesis and maintenance of cardiovascular, metabolic, and inflammatory diseases (9). Indeed, these small vesicles, released from plasma membrane of activated or apoptotic cells, carry proteins, nucleic acids and lipids that can modify phenotype and function when delivered to target cells (21). In particular, we have previously described that MPs from both apoptotic T cells and from metabolic syndrome patients induced endothelial dysfunction characterized by a decrease of nitric oxide (NO \cdot) release associated with the inhibition of endothelial NO-synthase (eNOS), and an increase in oxidative and nitrative stresses in human endothelial cells (2, 25). In addition, when MPs from either apoptotic T cells or metabolic syndrome patients were injected into mice, an impairment of endothelium-dependent vasorelaxation in response to acetylcholine was observed illustrating their pathophysiological relevance (2, 25). However, the molecular and cellular mechanism(s) underlying in the effects of MPs remain to be elucidated.

Several reports have shown that the activation of endoplasmic reticulum

(ER) stress response plays an important role in the pathogenesis of metabolic disorders such as insulin resistance, type 2 diabetes and obesity in animals (3, 26) as well as in humans (5). ER stress is induced by the accumulation of misfolded proteins in the ER lumen which leads to the activation of unfolded protein response (UPR). UPR is initiated by three main ER transmembrane stress sensors: pancreatic endoplasmic reticulum kinase (PERK), inositol-requiring enzyme 1 alpha (IRE1 α), and activating transcription factor 6 (ATF6) (7). The UPR is initially activated as a pro-survival mechanism, however, prolonged UPR activation in conditions such as obesity and metabolic syndrome leads to apoptosis, oxidative stress, and inflammation and is referred to as the "ER stress response". Recently, Galán et al (10) have demonstrated that chemical induction of ER stress with tunicamycin is associated with endothelial dysfunction and increased oxidative stress in the arterial wall. Under pathophysiological conditions such as hypertension, ER stress was reported to be involved in endothelial dysfunction induced by angiotensin II infusion (12). Furthermore, several lines of evidence strongly support the link between mitochondrial dysfunction and cardiovascular complications associated with metabolic syndrome. In the skeletal muscle of type 2 diabetic patients, a downregulation of PGC1 alpha-responsive genes involved in oxidative phosphorylation has been described (24). Also, both basal and maximal ADP-stimulated respirations were decreased in type 2 patients (22, 28). Similar results have been observed in human cardiac muscle (23). Moreover, an important increase in ER-mitochondria contact sites via the mitochondria-associated membranes (MAMs) have been described during high-fat diet-induced obesity leading to significant increase in hepatic lipid accumulation and decreased mitochondrial oxidative function (3). In parallel, elevated reactive oxygen species (ROS) production in cytosol, through the overexpression of the NADPH isoform NOX4, and in mitochondria have been detected in smooth muscle aortic cells from atherosclerotic aged donors leading to impaired mitochondrial function (32).

The aim of the present study is to decipher how MPs transfer their message to induce endothelial dysfunction. Detailed analyses of the

mechanisms involved with special interest in the cross-talk between ER and mitochondria in the regulation of oxidative stress were conducted. This would help underpinning new molecular and cellular pathways governing the vascular effects of MPs and will pave the way for identifying novel potential targets against MP-induced endothelial dysfunction, which predisposes to the initial pro-atherosclerotic events transforming metabolic syndrome to different vascular diseases.

Results

T lymphocytic MPs induce endothelial dysfunction through ER stress response activation

In response to treatment by MPs from apoptotic lymphocytes, UPR pathway activation was assessed using the ER stress inhibitor tauroursodeoxycholic acid (TUDCA), a chemical chaperone known to enhance adaptive response of ER. MPs activated the three canonical pathways associated with ER stress response: PERK, IRE1 α and ATF6. Indeed, MPs resulted in an increased phosphorylation of PERK and eIF2 α , as well as mRNA (not shown) and protein CHOP expressions (Fig. 1A-C). In addition, MP treatment enhanced X-box binding protein 1 (XBP1) splicing downstream to IRE1 α (Fig. 1D) and induced the nuclear translocation of ATF6 (Fig. 1E). Importantly, all these MP-evoked effects were prevented in the presence of the ER stress inhibitor TUDCA (Fig 1A-E). It should be noted that the ER stress inducer tunicamycin was able to activate the same three classical ER stress pathways, which were partially prevented by TUDCA (Fig. S1). Altogether, these data indicate that MPs from apoptotic lymphocytes lead to the activation of all three arms of ER stress response.

In order to verify whether ER stress response activation accounts for the endothelial dysfunction induced by T lymphocyte MPs (25), *in vitro* NO·

production was evaluated in the absence or the presence of TUDCA. As previously described, T lymphocyte MPs significantly decreased NO \cdot production in human aortic endothelial cells (HAoECs) (Fig. 1F). Interestingly, the inhibition of ER stress with TUDCA abolished the ability of MPs to reduce NO \cdot production. In order to establish the pathophysiological relevance of MPs, endothelium-dependent relaxation in response to acetylcholine was evaluated following MP incubation with mouse aortic rings in the absence or in the presence of TUDCA. MPs significantly reduced the maximal acetylcholine-evoked relaxation, which was improved by TUDCA (Fig. 1G). Finally, similarly to MPs, tunicamycin was able to reduce both *in vitro* NO \cdot release by endothelial cells and acetylcholine-induced relaxation of mouse aortic rings. These effects were partially prevented in the presence of TUDCA (Fig. S1).

Collectively, these results indicate that the activation of ER stress response is implicated in endothelial dysfunction induced by T lymphocyte MPs.

Involvement of membrane receptors in T lymphocyte MP-induced ER stress in endothelial cells

We have previously shown that T lymphocyte MPs, through their Fas-Ligand (FasL), induce vascular smooth muscle cell inflammation by directly interacting with Fas of the recipient cells (31). Also, Yang et al (33) have reported the involvement of low density lipoprotein receptor (LDL-R) in the effects induced by T lymphocyte MPs on human retinal endothelial cells. In order to determine the mechanism(s) by which MPs would induce ER stress in HAoECs, the implication of both Fas/FasL interaction and LDL-R was analyzed on MP-induced eIF2 α phosphorylation. Interestingly, we observed that neutralizing either FasL on MPs or LDL-R on endothelial cells significantly reduced the MP-induced phospho-eIF2 α (Fig. 2A). Altogether, these data indicate that both Fas/FasL interaction and LDL-R pathway are involved in MP-mediated ER stress induction.

Neutral sphingomyelinase (SMase) is the link between MP-activated receptor and ER stress response induction

Since SMase cascade has been implicated in the regulation of ER stress response (15), we assessed the involvement of SMase on MP-induced effects. MP treatment induced an increase of neutral SMase expression, which was prevented after neutralizing FasL on MPs (Fig. 2B) or when LDL-R on endothelial cells was blocked (Fig. 2C). Treatment of endothelial cells by MPs for 24 hours, but not for 4 hours, increased phospho-eIF2 α . Interestingly, silencing neutral SMase with a specific siRNA abolished MP-induced increase of eIF2 α phosphorylation after 24 hours of MP treatment (Fig. 2D and 2E).

Moreover, using either the specific neutral SMase inhibitor GW4869 or siRNA against neutral SMase completely prevented the MP-induced reduction of eNOS activity as reflected by phospho-Ser eNOS/phospho-Thr eNOS ratio (Fig. 2F and 2G). Furthermore, MP-induced NO \cdot reduction was abolished when neutral SMase was inhibited with GW4869 or silenced by siRNA (Fig 2H). Altogether, these results suggest that neutral SMase pathway controls the effects of MPs via Fas/FasL and LDL-R interaction upstream of ER stress, eNOS activation and NO \cdot production.

Cytosolic ROS production is upstream of T lymphocyte MP-induced ER stress in endothelial cells

The possible involvement of oxidative stress in T lymphocyte MP-induced ER stress activation was then assessed by incubating HAoECs with various inhibitors the sources of ROS prior to MP stimulation. Indeed, intracellular enzymatic systems with the capacity to generate ROS were inhibited by allopurinol, apocynin, rotenone, or N ω -nitro-L-arginine (L-NA) which are inhibitors of xanthine oxidase, NADPH oxidase, respiratory chain complex I, and NOS, respectively. At 24 hours of treatment, none of the ROS inhibitors modified the phosphorylation of eIF2 α in the absence of MPs (Fig. 3A). By contrast, all the inhibitors significantly decreased eIF2 α phosphorylation induced by MP treatment. These results suggest that MP-induced ROS production from different sources is required for the activation of ER stress response (Fig. 3B).

In order to establish the implication of cytoplasmic and mitochondrial ROS

in the effects of MPs, time course (i.e., 2, 4, and 24 hours) changes of ROS levels were measured. Analysis of ROS levels, using electronic paramagnetic resonance (EPR) and dihydroetidium (DHE) labeling, showed that T lymphocyte MPs had no effect on ROS production at 2 hours, increased at 4 hours and returned to basal levels at 24 hours (Fig 3 C-I). This effect of T lymphocyte MPs on ROS production was not affected by TUDCA. It is important to note that tunicamycin treatment induced similar patterns of ROS production as those obtained with MPs (Fig. S2). Interestingly, except for the mitochondrial ROS scavenger (mito-TEMPO), all of the ROS inhibitors tested (allopurinol, apocynin, rotenone and L-NA), reduced the early increase of cytosolic ROS production (Fig. 3J). To further analyze the enzyme involved in this ROS production, we found that lymphocyte MPs increased the expression of p47phox expression, a regulatory subunit of NADPH oxidase at 4 hours, but not at 24 hours of treatment (Fig. 3K). This increase was partially prevented after silencing of neutral SMase (Fig. 3K).

Altogether, lymphocyte MPs activate neutral SMase and induce an early increase of cytosolic ROS production, upstream of ER stress activation via at least the NADPH oxidase activation.

Cross-talk between ER and mitochondria is involved in the effects induced by lymphocyte MPs in endothelial cells

To monitor mitochondrial ROS production, MitoSox probe was used. Quantification of confocal images showed that mitochondrial ROS fluorescence was reduced at 2 and 4 hours, but was greatly enhanced after 24 hours of lymphocyte MP treatment (Fig. 4A-D). Interestingly, the ER stress inhibitor TUDCA did not modify the reduction of MitoSox fluorescence at 2 and 4 hours but completely abolished the increase at 24 hours. These results suggest that lymphocyte MPs induce a late increase of mitochondrial ROS by a mechanism downstream of ER stress activation. In order to confirm this, the mitochondrial ROS scavenger mito-Tempo was used and did not show any effect on the increase of phospho-eIF2 α induced by lymphocyte MPs (Fig. 4E).

The effects of MPs on mitochondrial O₂ consumption were then analyzed in order to decipher the role of mitochondria on the MP-induced endothelial dysfunction. Basal O₂ consumption was not modified either by MPs or MPs + TUDCA (Fig. 4F). However, MP treatment significantly reduced both oligomycin and FCCP mitochondrial respirations which were abolished when ER stress was inhibited with TUDCA (Fig. 4G and 4H). These findings suggest that MPs are able to modify mitochondrial respiration by a mechanism implicating ER stress. Exposure to MPs resulted in an increase of complex IV activity (Fig. 4I) but had no effect on the activity of the other complexes of the electron transport chain (not shown). To confirm the interaction between ER and mitochondria through the formation of tight physical junctions, MAM integrity was analyzed following MP treatment. As shown in Figure 4J and 4K, MPs induced MAM disruption characterized by an overexpression of mitofusin 2 (Mfn2) and a decreased expression of voltage-dependent anion channel 1 (VDAC1). Moreover, these effects were prevented in the presence of the ER stress inhibitor TUDCA suggesting that MP-induced ER stress leads to MAM disruption on endothelial cells. Finally, to verify whether the MP effects on mitochondria lead to endothelial dysfunction, NO[•] production was measured in the presence of mito-Tempo. Scavenging mitochondrial ROS with mito-Tempo abolished the decrease in NO[•] release induced by MPs (Fig. 4L). This result suggests that alteration of mitochondrial function with respect to respiration and ROS production, as a consequence of ER stress, leads to endothelial dysfunction.

MPs from metabolic syndrome patients induce endothelial dysfunction via Fas/FasL pathway and neutral SMase activation leading to ER stress activation in vitro and ex vivo

We have previously described that MPs from metabolic syndrome patients, but not those of non-metabolic syndrome subjects, induced endothelial dysfunction (2). Here, we tested whether molecular pathways involved in the effects of MPs from metabolic syndrome required also the cross-talk between ER and mitochondria and oxidative stress similarly to lymphocyte MPs. Therefore, MPs from metabolic syndrome patients or

non-metabolic syndrome subjects were isolated for whom detailed clinical information is described in Supplementary Table 1. As expected, metabolic syndrome patients showed greater visceral obesity as given by waist circumference, enhanced triglyceridemia, and increased blood pressure.

The total number of circulating MPs was significantly increased in patients with metabolic syndrome compared to non-metabolic syndrome subjects (Supplementary Table 2). Phenotypical characterization of cellular origin of MPs showed an increase of ~6-fold (annexin V⁺), ~3.3-fold (CD41⁺), and ~9.6-fold (CD146⁺) of the circulating level of procoagulant-, platelet-, and endothelial-derived MPs in metabolic syndrome patients compared to non-metabolic syndrome subjects, respectively. Also, levels of erythrocyte- and leukocyte-derived MPs (CD235a⁺, CD45⁺) were elevated (~9 and ~2.7-fold, respectively) in these patients.

As shown in Fig. 5A and 5B, MPs from metabolic syndrome patients, but not from non-metabolic syndrome individuals, induced an increase in phosphorylation of eIF2 α and nuclear translocation of ATF6, which were prevented in the presence of TUDCA. Similarly and as expected, MPs from metabolic patients, in comparison to non-metabolic syndrome subjects, caused a reduction in NO \cdot release from endothelial cells, which was abolished when ER stress was inhibited by TUDCA (Fig. 5C). Moreover, incubation of mouse aortic rings with MPs from metabolic syndrome patients, but not from non-metabolic syndrome subjects, was associated to a reduced endothelium-dependent relaxation in response to acetylcholine (Fig. 5D). This effect was prevented when vessels were incubated in the presence of TUDCA. Taken together, these results indicate that ER stress plays a key role in the induction of endothelial dysfunction induced by MPs from metabolic syndrome patients.

In order to establish the receptor involved in the effects of MPs from metabolic syndrome patients on endothelial cells, we neutralized either FasL on MPs or LDL-R on HAoECs. Interestingly, neutralization of FasL but not LDL-R on HAoECs, prevented the phosphorylation of eIF2 α by

metabolic syndrome MPs (Fig. 5E) and abolished their ability to enhance the expression of SMase (Fig. 5F). Finally, it is important to note that silencing neutral SMase with siRNA significantly abolished the increase of eIF2 α phosphorylation by metabolic syndrome MPs both at early (4 hours) and late stage (24 hours) of treatment (Fig. 5G and 5H), in contrast to T lymphocyte MPs which were able to increase eIF2 α at 24 hours only (Fig. 2E).

Cytosolic and mitochondrial ROS productions are downstream of metabolic syndrome MP-induced ER stress in endothelial cells

As illustrated in Figure 6A-H, MPs from metabolic syndrome induced an oxidative stress by increasing both cytosolic and mitochondrial ROS. DHE staining showed that MPs from metabolic syndrome patients, in comparison to non-metabolic syndrome subjects, enhanced cytosolic ROS at 2 and 4 hours, but not at 24 hours (Fig. 6A-D). Also, MPs from metabolic syndrome patients but not those from non-metabolic syndrome subjects increased MitoSox fluorescence at 24 hours, but not at 2 or 4 hours of treatment of HAoECs (Fig. 6E-H). Cytosolic ROS, but not mitochondrial ROS production, was abolished in the presence of ER stress inhibitor TUDCA. Interestingly, MPs induced p47phox expression at 4 hours, but not at 24 hours, which was abolished after SMase silencing (Fig. 7A and 7B). These results suggest that MPs from metabolic syndrome patients activate neutral SMase and induce a spatio-temporal increase of cytosolic ROS at early stage via the NADPH oxidase that concur to ER stress and mitochondrial ROS at late stages of stimulation. All of these effects participate to metabolic syndrome MP-induced endothelial dysfunction.

Discussion

In the present study, we provide evidence to support the crucial role of ER

and mitochondria interaction in the deleterious effects of human MPs on endothelial function. Most in detail, MPs from apoptotic T cells act on Fas and LDL-R, then, via neutral SMase cascade induce cytosolic ROS production which activates ER stress. Through the interaction between ER and mitochondria, mitochondrial ROS are increased and contribute to decreased bioavailability of NO \cdot and the subsequent impairment of endothelium-dependent vasorelaxation. Concerning MPs from metabolic syndrome patients, Fas/FasL, but not LDL-R, participates in the response induced by MPs. In addition, neutral SMase activation induces directly ER stress which, in turn, increases both cytosolic and mitochondrial ROS. All of these events lead to reduction of NO \cdot release and the subsequent impairment of endothelium-dependent vasorelaxation.

MPs have been described as cargo to delivery biological information between cells. We have previously described that MPs from either apoptotic T cells or metabolic syndrome patients induce endothelial dysfunction through the inhibition of eNOS (2, 25). In the present study, we show that both types of MPs induce endothelial dysfunction by ER stress activation. Thus, in a similar manner to tunicamycin, MPs activate the three canonical UPR pathways as illustrated by the increased phosphorylation of PERK and eIF2 α , XBP1 splicing and nuclear ATF6 translocation. ER stress activation has been described in endothelial cells of obese patients (11) and after an intralipid infusion in endothelial cells from healthy subjects (30), suggesting that metabolic disorders can lead to ER stress that may be relevant to vascular diseases. In the present study, the involved mechanisms in the ER induction of MPs from T cells and those from metabolic syndrome patients were found to be slightly different, probably due to the differences between MP origins. Indeed, we show that metabolic syndrome patients display elevated levels of platelet- and non-platelet-derived MPs, mainly from leukocytes, erythrocytes and endothelial cells. In this respect, we have previously shown that the effects of metabolic syndrome MPs on endothelial cells are probably supported by non-platelet-derived MPs since this subset of MPs reduce NO \cdot production (2). In addition, Chironi et al (6) have found that circulating levels of leukocyte-derived MPs were higher in metabolic syndrome

patients than in healthy individuals and that these levels positively correlate with the number of metabolic syndrome components.

MPs carry proteins, lipids and nucleic acids, mainly mRNA and miRNA. Since RNase treatment has no effect in MP-induced responses on HAOECs (not shown), we decided to analyze the direct interaction between MPs and target cells via the ligand-receptor binding. We have previously shown that interaction of FasL carried by MPs with Fas at the surface of target cells mediates the induction of pro-inflammatory proteins in the vascular wall (1, 31), whereas Yang et al(33) demonstrated the involvement of LDL-R in the MP-induced effects. Here, we show that both mechanisms participate to the effects of MPs from T cells, but only Fas/FasL interaction is involved in the effects generated by MPs from metabolic syndrome patients. Indeed, neutralization of LDL-R on endothelial cells does not affect metabolic syndrome MP-induced ER stress. Nevertheless, both types of MPs are able to activate neutral SMase which has been directly related to endothelial dysfunction (for review see 27). In addition, we provide proof that inhibition of neutral SMase, or silencing its expression, strongly blocks MP-induced ER stress and improves both eNOS activity and NO[•] production, illustrating the implication of neutral SMase pathway on MP-induced endothelial dysfunction.

Nonetheless, intracellular pathways involved in the effects of both types of MPs show differential spatial and temporal regulation with respect to cytosolic and mitochondrial pools of ROS. Activation of ER stress by MPs from T cells is dependent on ROS production from different origins since inhibitors of NADPH oxidase, xanthine oxidase, and mitochondrial complex I prevented phosphorylation of eIF2 α , which suggests a link between the different ROS sources. Thus, it has been proposed that NADPH oxidase plays a central role in orchestrating the activation and dysfunction of other enzymes generating ROS (for review see 14). In addition, the early increase (at 4 hours of treatment) on cytosolic ROS production evoked by MPs from apoptotic T cells was not inhibited by TUDCA, indicating that the enhancement of cytosolic ROS is upstream to

ER stress. Interestingly, silencing SMase partially prevented the increase of p47phox subunit of NADPH oxidase induced by MPs at 4 hours suggesting that SMase activation precedes NADPH oxidase-dependent deleterious effects of MPs in endothelial cells. The SMase-p47phox-ROS cascade has been described in vascular smooth muscle cells under hypoxia conditions (8) and in neurons exposed to TNF- α (4), however, to the best of our knowledge, the relationship of this cascade with ER stress has never been studied. Furthermore, several studies showed that cellular toxics such as arsenic or ischemia/reperfusion injury exert their cytotoxicity by inducing apoptosis through a ROS-induced ER stress which is associated to a mitochondrial dysfunction (29, 34). In the present study, we provide evidence that mitochondrial ROS increase, changes on mitochondrial respiration and complex IV activity are detected at late (24 hours) but not early (4 hours) MP treatment, and are abolished when ER stress is inhibited, indicating that ER stress activation is mandatory for the generation of mitochondrial ROS and perturbation of mitochondrial function. Remarkably, scavenging of mitochondrial ROS by mito-Tempo restores NO \cdot production, illustrating the involvement of mitochondrial ROS on the MP-induced endothelial dysfunction. Moreover, the enhanced MAM alteration, which suggests an interaction between ER stress and mitochondria, could account for the subsequent modifications of the mitochondrial function. It is worth noting that ER and mitochondrial cross-talk has been described in neurodegenerative (13) and metabolic disorders (3, 18) suggesting that rescuing mitochondrial and ER stress impairments may identify new targets against these pathologies.

In this respect, activation of SMase pathway by MPs from metabolic syndrome patients directly induces ER stress which on its turn evokes an increase of both cytosolic and mitochondrial ROS. It is important to note that the spatio-temporal regulations of ROS induced by MPs from metabolic syndrome patients are different from those of T lymphocytic MPs. In fact, with respect to the increase of cytosolic ROS, ER stress activation is downstream for the former and upstream for the latter. This differential response probably results from the fact that a mixture of MP subsets triggers the effects of metabolic syndrome MPs although we

previously reported that non-platelet MPs are responsible for endothelial dysfunction. Indeed, it is well known that the content of MPs depends on the cells they originate from, the stimulus of production and the mechanism of vesicle generation (9).

The difference in the mechanism involved in ER stress response induced by T lymphocytic MPs and those from metabolic syndrome patients might explain the different level of endothelial dysfunction induced by both types of MPs. We have no evidence of any NOS uncoupling nor diminished levels of tetrahydrobiopterin in the present study, but it is most likely that reduced acetylcholine-induced relaxation is due to spatio-temporal increase of oxidative stress that leads to reduced NO production. However, we cannot exclude that mechanisms other than NO pathway, such as cyclo-oxygenase pathways, might be involved. Nevertheless, the present study emphasizes the importance of ER stress as a key control of oxidative stress leading to endothelial dysfunction by both types of MPs. In this respect, it has been described that the presence of unfolded proteins in the ER lumen is sufficient to activate oxidative stress (for review see 19). This process may be related with the fact that ER stress induction by MPs from metabolic syndrome patients takes place early, only after 4 hours of MP treatment.

Collectively, we demonstrate that endothelial dysfunction triggered by MPs involves temporal cross-talk between ER and mitochondria with respect to spatial regulation of oxidative stress via the SMase route (Figure 8). These events occur via interaction of MPs on endothelial cells with Fas and/or LDL-R. These results highlight novel potential targets to fight against the pivotal role of MPs on endothelial dysfunction leading to the increase of cardiovascular complications including those associated with metabolic syndrome.

Innovation

In last years, an increasing interest on circulating microparticles, extracellular vesicles released from plasma membrane of cells, as players in the development and maintenance of cardiovascular diseases

has been reported. Our study identifies a new pathway involving a spatio-temporal cross-talk between endoplasmic reticulum and mitochondria in the generation of oxidative stress accounting for the impairment of endothelial function induced by microparticles from metabolic syndrome patients and allow identification of potential therapeutic targets to treat vascular complications associated with metabolic diseases.

Materials and Methods

MP production from T-cells. The human lymphoid CEM T-cell line was used for MP production. Cells were seeded at 10^6 cells/ml and cultured in serum-free X-VIVO 15 medium (Lonza, Basel, Switzerland). MPs were produced as previously described (20, 25). Briefly, cells were treated with actinomycin D ($1 \mu\text{g/ml}$; Sigma-Aldrich, St Quentin-Fallavier, France) for 24 hours. The supernatant was obtained by centrifugation at $750g$ for 15 minutes, and then at $1,500g$ for 5 minutes to remove cells and large debris, respectively. MPs from the supernatant were washed after three centrifugation steps (45 minutes, $14,000g$) and recovered in $400 \mu\text{l}$ of sterile NaCl 0.9%. Last washing medium was used as vehicle. The determination of the amount of MPs was conducted by measuring MP-associated proteins using the DC Protein Assay (Bio-Rad, Hercules, CA). MPs were used at $10 \mu\text{g/ml}$ corresponding to $1,330 \pm 312 \times 10^3$ MPs. This concentration of lymphocyte MPs is found in plasma from patients undergoing carotid endarterectomy ($0-2 \times 10^6$ MPs/ml plasma) (16).

Metabolic syndrome patients. This study was approved by the ethics committee of the University Hospital of Angers (France) (NCT: 00997165). A total of 30 patients were included with metabolic syndrome from the METABOL cohort at the Department of Endocrinology and Nutrition of the University Hospital of Angers. Patients were eligible for inclusion, according to the National Cholesterol Education Program-Adult Treatment Panel III, when they had at least three of the following five criteria : i) waist

circumference >102 or 88 cm for men and women, respectively; ii) systolic and diastolic pressures \geq 130/85 mmHg; iii) fasting glycemia \geq 1.1 g/l; iv) triglycerides \geq 1.5 g/l; and v) high-density cholesterol lipoprotein <0.4 g/l in men or <0.5 g/l in women (Supplementary Table 1). Patients with a history of cardiovascular diseases, preexistent chronic inflammatory disease, and cancer were excluded. Normal controls consisted of 20 subjects who met less than two of the metabolic syndrome criteria (70% without any component of metabolic syndrome).

MP collection from patients. Peripheral blood (20 ml) from non-metabolic syndrome or metabolic syndrome subjects was collected in EDTA tubes (Vacutainers; Becton Dickinson, Le Pont de Claix, France) from a peripheral vein using a 21-gauge needle to minimize platelet activation and was processed within 2 hours. After a 20-minute centrifugation at 270g, platelet-rich plasma was separated from whole blood which was then centrifuged for 20 minutes at 1500g to obtain platelet-free plasma (PFP). Two hundred μ l of PFP were frozen and stored at -80°C until subsequent use for MP characterization by flow cytometry. Remaining PFP was subjected to three series of centrifugations each at 21,000g for 45 minutes to pellet MPs for *in vitro* studies, and the supernatant was replaced by 200 μ l of sterile 0.9% NaCl and stored at 4°C until subsequent use. MPs from non-metabolic syndrome or metabolic syndrome subjects were used at the circulating concentration detected for each individual, as previously described (1, 2).

Characterization of MP phenotype. Membrane MP sub-populations were discriminated in PFP according to the expression of membrane-specific antigens (1, 2). Irrelevant human IgG was used as an isotype-matched negative control for each sample. For numeration studies, 10 μ l of PFP were incubated with 5 μ l of specific antibody (Beckman Coulter, Villepinte, France). Annexin V binding was used to numerate phosphatidylserine-expressing circulating MPs (2 μ l of annexin V/5 μ l PFP). After 30 minutes at room temperature, samples were diluted in 300 μ l of sterile 0.9% NaCl or annexin-V labeling buffer, respectively. Then, an equal volume of sample and Flowcount beads were added and samples were analyzed in a

flow cytometer 500 MPL system (Beckman Coulter).

Cell culture. Human Aortic Endothelial Cells (HAoECs) were maintained in culture in endothelial cell growth medium MV2 (Promocell, Heidelberg, Germany) supplemented with 1% streptomycin/penicillin (Lonza). Cells were treated for 24 hours with ER stress inducer tunicamycin (0.8 $\mu\text{g/ml}$, Sigma-Aldrich), 10 $\mu\text{g/ml}$ of T lymphocyte MPs or those from non-metabolic syndrome or metabolic syndrome subjects, in the absence or in the presence of the ER stress inhibitor, TUDCA (100 $\mu\text{mol/l}$, Sigma-Aldrich). In another set of experiments, 30 minutes before MP treatment, cells were pre-treated with the NADPH oxidase inhibitor, apocynin (Apo, 100 $\mu\text{mol/l}$, Calbiochem, Darmstadt, Germany), the inhibitor of xanthine oxidase, allopurinol (Allo, 50 $\mu\text{mol/l}$, Sigma-Aldrich), the inhibitor of mitochondrial complex I NADH dehydrogenase, rotenone (Rot, 5 $\mu\text{mol/l}$, Sigma-Aldrich), the NO \cdot synthase inhibitor, L-NA (100 $\mu\text{mol/l}$, Sigma-Aldrich), the mitochondria-targeted scavenger mito-TEMPO (25 nmol/l, Santa Cruz Biotechnology) or the inhibitor of neutral SMase, GW4869 (10 $\mu\text{mol/l}$, [PubMed](#) mol/l, Sigma-Aldrich). All products were used at concentrations at which no cytotoxicity was observed, as deduced from trypan blue exclusion assay.

Western Blot. After treatment, cells were homogenized and lysed. Proteins (40 μg) were separated on 4-12% NuPage gels (ThermoFisher Scientific, Rockford, IL). Blots were probed with antibodies against PERK, phospho-PERK, eIF2 α , phospho-eIF2 α , CHOP, phospho-Thr495 eNOS (Cell Signaling, Danvers, MA), mitofusin 2 (Mfn2), VDAC1 α (Abcam, Cambridge, United Kingdom), p47-phox and phospho-Ser1177 eNOS (BD Biosciences, San Jose, CA). A polyclonal mouse anti-human β -actin antibody (Sigma-Aldrich) was used for standardization of protein gel loading.

In another set of experiments, cells were pre-treated with LDL-R antibody (5 $\mu\text{g/ml}$, R&D Systems, Minneapolis, MN) or its control IgG antibody for 30 minutes before MP treatment. Also, FasL carried by MPs was pre-incubated with human anti-FasL (5 μg , BD Biosciences) for 30 minutes at

4°C to allow neutralization of MP FasL after being washed two times with NaCl 0.9% in order to remove unbound anti-FasL antibody.

Nuclear translocation of ATF6 by confocal microscopy. Cells were seeded on glass slides (Ibidi, Martinsried, Germany), for 24 hours and then treated with either tunicamycin or MPs for 24 hours in the absence or presence of TUDCA. Cells were then washed, and fixed with 4% paraformaldehyde. Then, cells were treated with 5% bovine serum albumin, permeabilized by 0.1% Triton, incubated with anti-ATF6 (Abcam) for 1 hour, followed by 1 hour incubation with Alexa fluo-546 secondary antibody (ThermoFisher Scientific) at room temperature. Finally, DAPI (300 mmol/l, Santa Cruz Biotechnology) was added for 5 minutes. Cells were washed and fluorescence was measured with a confocal microscopy (CLMS 700, Zeiss, ZEN software). All images were acquired using x40 objective.

Quantitative and semi-quantitative PCR. Cells were treated for 6 hours as described above and then, frozen cell pellets were used to investigate the expression of mRNA for CHOP by RT-PCR (human forward primer GAACGGCTCAAGCAGGAAAT, human reverse primer TTCACCATTTCGGTCAATCAGAG). Total RNA was isolated using miRNeasy Qiagen microkit (Hilden, Germany). cDNA was generated using PrimeScript™ RT reagent Kit (Takara/Clontech, Mountain View, CA) from 500 ng of RNA with random hexameric primers. RT-PCR analyses were performed using a CFX96™ Real-Time PCR Detection System and SYBR Green detection (Bio-Rad). Semi-quantitative PCR was made for the expression of XBP-1 (human forward primer AAACAGAGTAGCAGCTCAGACTGC, human reverse primer TCCTTCTGGGTAGACCTCTGGGAG) by using PTC-200 (MJ Research, St Bruno, Canada). β -Tubulin was used as the house keeping reference gene.

siRNA transfection. Transient transfection of HAoECs was done according to the manufacturer's protocol (Santa Cruz Biotechnology). Briefly, HAoECs were treated with either control siRNA or neutral SMAse siRNA

for 6 hours in a serum- and antibiotic-free medium. Cells were then washed and normal fresh medium was added for 24 hours before treatment with MPs for 24 hours.

NO[•] measurement. After treatment for 24 hours, as described above, cells were loaded with 4, 5-diaminofluorescein diacetate (DAF-2DA, Santa Cruz Biotechnology) (10 $\mu\text{mol/l}$) for 30 minutes at 37°C, and fluorescence was measured.

Endothelial function. Aortic rings were obtained from male Swiss mice bred at the animal facility at the University of Angers. After 24 hours of MP incubation, aortic rings were mounted on a wire myograph filled with physiological salt solution, as previously described (20). Endothelium-dependent vasodilatation was studied by cumulative application of acetylcholine (1 nmol/l-10 $\mu\text{mol/l}$, Sigma-Aldrich) in aortas with functional endothelium precontracted with U46619 (Sigma-Aldrich).

Anion superoxide determination by EPR studies. The detection of anion superoxide production was performed by EPR technique using 1-hydroxy-3-methylcarbonyl-2, 2, 5, 5 tetramethyl pyrrolidine (CMH) (Noxygen, Mainz, Germany) as spin trap. Briefly, after 24 hours of treatment, the medium was replaced with 500 μl of deferoxamine-chelated Krebs-Hepes solution containing CMH (500 $\mu\text{mol/l}$), deferoxamine (25 $\mu\text{mol/l}$, Sigma-Aldrich), and sodium diethylthiocarbamate (5 $\mu\text{mol/l}$, Sigma-Aldrich), and incubated for 45 minutes at 37°C. ROS measurement was performed on a table-top x-band spectrometer Miniscope (MS200; Magnettech, Berlin, Germany). Recordings were made at 77°K, using a Dewar flask. Instrument settings were 10 mW of microwave power, 1 mT of amplitude modulation, 100 kHz of modulation frequency, 150 seconds of sweep time and three scans. The quantitative measurement of the $\text{O}_2^{\cdot-}$ signal amplitude was reported to the relative units for protein concentration (amplitude/ $\mu\text{g}/\mu\text{l}$).

ROS measurement by dihydroethidium (DHE) or MitoSox staining. Endothelial cells were grown on glass slides (Ibidi), and after different treatments, they were washed and then incubated with either the

oxidative fluorescent dye DHE (5 $\mu\text{mol/l}$, Sigma-Aldrich) for 30 minutes at 37°C or MitoSox red (5 $\mu\text{mol/l}$, ThermoFisher Scientific) for 10 minutes at 37°C. Then, cells were fixed by 4% paraformaldehyde for 20 minutes at room temperature. DAPI was added for 5 minutes. Finally, cells were visualized with confocal microscopy (CLMS 700, Zeiss, ZEN software). All images were acquired using an x63 objective.

Measurement of whole cell respiration. Respiration rates were measured in treated HAOECs. The cells were collected by trypsinization, washed once in culture medium and centrifuged (500g, 5 minutes). The pellet was resuspended in respiratory medium, corresponding to normal culture medium without FBS and antibiotics, both reagents known to interfere with mitochondrial respiration. Mitochondrial oxygen consumption was measured at 37°C using a high-resolution Oxygraph-2K respirometer (Oroboros, Innsbruck, Austria). Oxygraphy experiments were performed on cells cultured in T75 flasks, corresponding to an average of 5×10^6 cells per flask. Basal respiration rate of cells was determined by measuring the linear rate of oxygen consumption. Oligomycin (1 $\mu\text{g/ml}$) was then added to determine the non-phosphorylating respiration rate. The uncoupling respiration rate was also recorded by stepwise addition of FCCP (0.2-1 $\mu\text{mol/l}$) up to the optimal concentration representing the maximal capacity of the respiratory chain without the regulation of ATP synthase. Finally, the non-mitochondrial oxygen consumption rate was determined by adding antimycin A (1 $\mu\text{g/ml}$). At the end of the experiment, a standard volume of respiratory medium is collected and centrifuged for 2 minutes at 16,000g. The cell pellet was then resuspended in NaCl (0.9%) and protein concentration was determined spectrophotometrically. Respiration rates were expressed in nmoles of O_2 consumed per minute and per mg protein.

Mitochondrial enzyme activity measurements. The activity of the different mitochondrial respiratory chain complexes was measured on cell homogenates, at 37°C, using a SAFAS spectrophotometer (SAFAS, Monaco, France).

Statistics. Data are expressed as mean±SEM. Statistical analyses were performed by a one-way ANOVA and then Mann-Whitney U, or ANOVA for repeated measures and subsequent Bonferroni post hoc test. P<0.05 was considered to be statistically significant.

Acknowledgments

We thank M. Wertheimer and SCAHU staff (Université d'Angers) for taking care of animals, G. Hilairet for expert technical assistance for confocal microscopy, and the staff of Centre Hospitalo-Universitaire d'Angers for analysis of clinical data of METABOL cohort. This work was supported by Institut National de la Santé et de la Recherche Médicale, Université d'Angers and Centre Hospitalo-Universitaire d'Angers. ZS is recipient of a doctoral fellowship from the «Association de Spécialisation et d'Orientation Scientifique» from Lebanon.

List of Abbreviations

ADP: adenosine diphosphate

ATF6: activating transcription factor 6

CMH: 1-hydroxy-3-methylcarbonyl-2, 2, 5, 5 tetramethyl pyrrolidine

DHE: dihydroethidium

EDTA: ethylenediaminetetraacetic acid

eIF2 α : Eukaryotic translation initiation factor 2 α

eNOS: endothelial nitric oxide synthase

EPR: electronicparamagnetic resonance

ER: endoplasmic reticulum

FasL: Fas Ligand

HAoECs: human aortic endothelial cells

HRP: horseradish peroxidase

IRE1 α : inositol-requiring enzyme 1 alpha

LDL-R: low density lipoprotein receptor

L-NA: N ω -nitro-L-arginine

MAM: mitochondria-associated membranes

Mfn2: mitofusin 2

MPs: microparticles

NO \cdot : nitric oxide

PERK: pancreatic endoplasmic reticulum kinase

PFP: platelet-free plasma

PGC1: peroxisome proliferator-activated receptor gamma coactivator 1

ROS: reactiveoxygen species

SMAse: sphingomyelinase

TUDCA: sodium tauroursodeoxycholate

UPR: unfolded protein response

VDAC1: voltage-dependent anion channel 1

XBP1: x-box binding protein 1

References

1. Agouni A, Ducluzeau PH, Benameur T, Faure S, Sladkova M, Duluc L, Leftheriotis G, Pechanova O, Delibegovic M, Martinez MC, and Andriantsitohaina R. Microparticles from patients with metabolic syndrome induce vascular hypo-reactivity via Fas/Fas-ligand pathway in mice. *PLoS One* 6: e27809, 2011.
2. Agouni A, Lagrue-Lak-Hal AH, Ducluzeau PH, Mostefai HA, Draunet-Busson C, Leftheriotis G, Heymes C, Martinez MC, and Andriantsitohaina R. Endothelial dysfunction caused by circulating microparticles from patients with metabolic syndrome. *Am J Pathol* 173: 1210-1219, 2008.
3. Arruda AP, Pers BM, Parlakgöl G, Güney E, Inouye K, and Hotamisligil GS. Chronic enrichment of hepatic endoplasmic reticulum-mitochondria contact leads to mitochondrial dysfunction in obesity. *Nat Med* 20: 1427-1435, 2014.
4. Barth BM, Gustafson SJ, and Kuhn TB. Neutral sphingomyelinase activation precedes NADPH oxidase-dependent damage in neurons exposed to the proinflammatory cytokine tumor necrosis factor- α . *J Neurosci Res* 90: 229-242, 2012.
5. Boden G, Duan X, Homko C, Molina EJ, Song W, Perez O, Cheung P, and Merali S. Increase in endoplasmic reticulum stress-related proteins and genes in adipose tissue of obese, insulin-resistant individuals. *Diabetes* 57: 2438-2444, 2008.
6. Chironi G, Simon A, Hugel B, Del Pino M, Gariepy J, Freyssinet JM, and Tedgui A. Circulating leukocyte-derived microparticles predict subclinical atherosclerosis burden in asymptomatic subjects. *Arterioscler Thromb Vasc Biol* 26: 2775-2780, 2006.

7. Cominacini L, Mozzini C, Garbin U, Pasini A, Stranieri C, Solani E, Vallerio P, Tinelli IA, and Fratta Pasini A. Endoplasmic reticulum stress and Nrf2 signaling in cardiovascular diseases. *Free Radic Biol Med* 88: 233-242, 2015.
8. Frazziano G, Moreno L, Moral-Sanz J, Menendez C, Escolano L, Gonzalez C, Villamor E, Alvarez-Sala JL, Cogolludo AL, and Perez-Vizcaino F. Neutral sphingomyelinase, NADPH oxidase and reactive oxygen species. Role in acute hypoxic pulmonary vasoconstriction. *J Cell Physiol* 226: 2633-2640, 2011.
9. Gaceb A, Martinez MC, and Andriantsitohaina R. Extracellular vesicles: new players in cardiovascular diseases. *Int J Biochem Cell Biol* 50: 24-28, 2014.
10. Galán M, Kassan M, Kadowitz PJ, Trebak M, Belmadani S, and Matrougui K. Mechanism of endoplasmic reticulum stress-induced vascular endothelial dysfunction. *Biochim Biophys Acta* 1843: 1063-1075, 2014 [PubMed](#) .
11. Kaplon RE, Chung E, Reese L, Cox-York K, Seals DR, and Gentile CL. Activation of the unfolded protein response in vascular endothelial cells of nondiabetic obese adults. *J Clin Endocrinol Metab* 98: E1505-E1509, 2013.
12. Kassan M, Galán M, Partyka M, Saifudeen Z, Henrion D, Trebak M, and Matrougui K. Endoplasmic reticulum stress is involved in cardiac damage and vascular endothelial dysfunction in hypertensive mice. *Arterioscler Thromb Vasc Biol* 32: 1652-1661, 2012.
13. Kaus A, and Sareen D. ALS patient stem cells for unveiling disease signatures of motoneuron susceptibility: perspectives on the deadly mitochondria, ER stress and calcium triad. *Front Cell Neurosci* 9: 448, 2015.
14. Konior A, Schramm A, Czesnikiewicz-Guzik M, and Guzik TJ. NADPH oxidases in vascular pathology. *Antioxid Redox Signal* 20: 2794-2814, 2014.

15. Kucuksayan E, Konuk EK, Demir N, Mutus B, and Aslan M. Neutral sphingomyelinase inhibition decreases ER stress-mediated apoptosis and inducible nitric oxide synthase in retinal pigment epithelial cells. *Free Radic Biol Med* 72: 113-123, 2014.
16. Leroyer AS, Isobe H, Lesèche G, Castier Y, Wassef M, Mallat Z, Binder BR, Tedgui A, and Boulanger CM. Cellular origins and thrombogenic activity of microparticles isolated from human atherosclerotic plaques. *J Am Coll Cardiol* 49: 772-777, 2007.
17. Liao JK. Linking endothelial dysfunction with endothelial cell activation. *J Clin Invest* 123: 540-541, 2013.
18. López-Crisosto C, Bravo-Sagua R, Rodriguez-Peña M, Mera C, Castro PF, Quest AF, Rothermel BA, Cifuentes M, and Lavandero S. ER-to-mitochondria miscommunication and metabolic diseases. *Biochim Biophys Acta* 1852: 2096-2105, 2015.
19. Malhotra JD, and Kaufman RJ. ER stress and its functional link to mitochondria: role in cell survival and death. *Cold Spring Harb Perspect Biol* 3: a004424, 2011.
20. Martin S, Tesse A, Hugel B, Martínez MC, Morel O, Freyssinet JM, and Andriantsitohaina R. Shed membrane particles from T lymphocytes impair endothelial function and regulate endothelial protein expression. *Circulation* 109: 1653-1659, 2004.
21. Mause SF, and Weber C. Microparticles: protagonists of a novel communication network for intercellular information exchange. *Circ Res* 107: 1047-1057, 2010.
22. Mogensen M, Sahlin K, Fernström M, Glintborg D, Vind BF, Beck-Nielsen H, and Højlund K. Mitochondrial respiration is decreased in skeletal muscle of patients with type 2 diabetes. *Diabetes* 56: 1592-1599, 2007.
23. Montaigne D, Marechal X, Coisne A, Debry N, Modine T, Fayad G,

Potelle C, El Arid JM, Mouton S, Sebti Y, Duez H, Preau S, Remy-Jouet I, Zerimech F, Koussa M, Richard V, Nevriere R, Edme JL, Lefebvre P, and Staels B. Myocardial contractile dysfunction is associated with impaired mitochondrial function and dynamics in type 2 diabetic but not in obese patients. *Circulation* 130: 554-564, 2014.

24. Mootha VK, Lindgren CM, Eriksson KF, Subramanian A, Sihag S, Lehar J, Puigserver P, Carlsson E, Ridderstråle M, Laurila E, Houstis N, Daly MJ, Patterson N, Mesirov JP, Golub TR, Tamayo P, Spiegelman B, Lander ES, Hirschhorn JN, Altshuler D, and Groop LC. PGC-1alpha-responsive genes involved in oxidative phosphorylation are coordinately downregulated in human diabetes. *Nat Genet* 34: 267-273, 2003.

25. Mostefai HA, Agouni A, Carusio N, Mastronardi ML, Heymes C, Henrion D, Andriantsitohaina R, and Martinez MC. Phosphatidylinositol 3-kinase and xanthine oxidase regulate nitric oxide and reactive oxygen species productions by apoptotic lymphocyte microparticles in endothelial cells. *J Immunol* 180: 5028-5035, 2008.

26. Ozcan L, Ergin AS, Lu A, Chung J, Sarkar S, Nie D, Myers MG Jr, and Ozcan U. Endoplasmic reticulum stress plays a central role in development of leptin resistance. *Cell Metab* 9: 35-51, 2009.

27. Pavoine C, and Pecker F. Sphingomyelinases: their regulation and roles in cardiovascular pathophysiology. *Cardiovasc Res* 82: 175-183, 2009.

28. Phielix E, Schrauwen-Hinderling VB, Mensink M, Lenaers E, Meex R, Hoeks J, Kooi ME, Moonen-Kornips E, Sels JP, Hesselink MK, and Schrauwen P. Lower intrinsic ADP-stimulated mitochondrial respiration underlies in vivo mitochondrial dysfunction in muscle of male type 2 diabetic patients. *Diabetes* 57: 2943-2949, 2008.

29. Sun Y, Pu LY, Lu L, Wang XH, Zhang F, and Rao JH. N-acetylcysteine attenuates reactive-oxygen-species-mediated endoplasmic reticulum stress during liver ischemia-reperfusion injury. *World J Gastroenterol* 20: 15289-15298, 2014.

30. Tampakakis E, Tabit CE, Holbrook M, Linder EA, Berk BD, Frame AA, Bretón-Romero R, Fetterman JL, Gokce N, Vita JA, and Hamburg NM. Intravenous lipid infusion induces endoplasmic reticulum stress in endothelial cells and blood mononuclear cells of healthy adults. *J Am Heart Assoc* 5: e002574, 2016.
31. Tesse A, Martínez MC, Hugel B, Chalupsky K, Muller CD, Meziani F, Mitolo-Chieppa D, Freyssinet JM, and Andriantsitohaina R. Upregulation of proinflammatory proteins through NF-kappaB pathway by shed membrane microparticles results in vascular hyporeactivity. *Arterioscler Thromb Vasc Biol* 25: 2522-2527, 2005.
32. Vendrov AE, Vendrov KC, Smith A, Yuan J, Sumida A, Robidoux J, Runge MS, and Madamanchi NR. NOX4 NADPH oxidase-dependent mitochondrial oxidative stress in aging-associated cardiovascular disease. *Antioxid Redox Signal* 23: 1389-1409, 2015.
33. Yang C, Gagnon C, Hou X, and Hardy P. Low density lipoprotein receptor mediates anti-VEGF effect of lymphocyte T-derived microparticles in Lewis lung carcinoma cells. *Cancer Biol Ther* 10: 448-456, 2010.
34. Yen YP, Tsai KS, Chen YW, Huang CF, Yang RS, and Liu SH. Arsenic induces apoptosis in myoblasts through a reactive oxygen species-induced endoplasmic reticulum stress and mitochondrial dysfunction pathway. *Arch Toxicol* 86: 923-933, 2012.

Figure 1: T lymphocytic microparticles (MPs) induce endoplasmic reticulum (ER) stress response. Effects of MPs on the three canonical arms of ER stress response. TUDCA was used to inhibit ER stress response. **(A-C)** Anti-phospho-PERK, anti-phospho-eIF2 α , anti-CHOP and anti- β actin antibody immunoblots of human aortic endothelial cells. **(D)** Semiquantitative PCR of XBP-1. **(E)** Immunofluorescent staining

showing the nuclear translocation of ATF6. **(F)** Nitric oxide (NO·) production measured by electronic paramagnetic resonance. **(G)** Endothelial-dependent vasorelaxation induced by acetylcholine (ACh) on mouse aortic rings. * $P < 0.05$, ** $P < 0.01$. For statistical analyses, one-way analysis of variance and Mann-Whitney U or analysis of variance for repeated measures and subsequent Bonferroni post hoc test for acetylcholine-induced vasorelaxation were used. $n = 3-4$.

Figure 2: ER stress response induced by T lymphocytic microparticles (MPs) is mediated by neutral sphingomyelinase (SMase) activation via Fas/Fas-Ligand interaction and LDL-receptor. (A-C) Effects of MPs on ER stress response (phospho-eIF2 α) and Smase expression are inhibited by anti-Fas-Ligand or LDL-receptor antibodies. **(D-H)** Pharmacological inhibition of SMase with GW4869 or silencing with siRNA abolished MP-induced ER stress response and endothelial dysfunction.* $P < 0.05$. For statistical analyses, one-way analysis of variance and Mann-Whitney U were used. $n = 3-4$.

Figure 3: Cytosolic production of reactive oxygen species by MPs is upstream of ER stress response. (A, B) Effects of 24 hours treatment with inhibitors of ROS sources on ER stress response (phospho-eIF2 α) in the absence **(A)** or in the presence of MPs **(B)**. **(C-I)** Cytosolic ROS production measured by electronic paramagnetic resonance (C-E) and DHE labeling (F-I). **(J)** Effects of inhibitors of ROS sources on ROS production after 4 hours of MP treatment. **(K)** Effects of silencing SMase on MP-induced p47phox expression. * $P < 0.05$, ** $P < 0.01$, *** $P < 0.001$. For statistical analyses, one-way analysis of variance and Mann-Whitney U were used. $n = 3-7$.

Figure 4: Mitochondrial production of reactive oxygen species by MPs is downstream of ER stress response. (A-D) Mitochondrial ROS production measured by MitoSox labelling. **(E)** Scavenging mitochondrial ROS with Mito-Tempo has not effect on ER stress response. **(F-I)** Effects of MPs on mitochondrial respiration and complex IV activity. **(J and K)** Effects of MPs on mitochondria-associated membranes. **(L)** Mito-Tempo

improves NO \cdot production induced by MPs. *P<0.05, **P<0.01. For statistical analyses, one-way analysis of variance and Mann-Whitney U were used. *n*=4-6.

Figure 5: Microparticles from metabolic syndrome patients (MetS MPs) induce endoplasmic reticulum (ER) stress response via Fas/Fas-Ligand interaction and neutral sphingomyelinase (SMase) pathway.

Effects of MPs from non-metabolic syndrome subjects (nMetS MPs) and MetS MPs on the canonical arms of ER stress response. TUDCA was used to inhibit ER stress response. **(A)** Anti-phospho-eIF2 α antibody immunoblots of human aortic endothelial cells. **(B)** Immunofluorescent staining showing the nuclear translocation of ATF6. **(C)** Nitric oxide (NO \cdot) production measured by electronic paramagnetic resonance.

(D) Endothelial-dependent vasorelaxation induced by acetylcholine (Ach) on mouse aortic rings. **(E and F)** Effects of MPs on ER stress response (phospho-eIF2 α) and SMase expression are inhibited by anti-Fas-Ligand antibodies. **(G and H)** Silencing SMase with siRNA abolished MP-induced ER stress response. *P<0.05, **P<0.01. For statistical analyses, one-way analysis of variance and Mann-Whitney U or analysis of variance for repeated measures and subsequent Bonferroni post hoc test for acetylcholine-induced vasorelaxation were used. *n*=3-4.

Figure 6: Cytosolic and mitochondrial production of reactive oxygen species (ROS) by MetS MPs are downstream of ER stress response.

(A-D) Cytosolic ROS production measured by DHE staining. **(E-H)** Mitochondrial ROS production measured by MitoSox labelling. For statistical analyses, one-way analysis of variance and Mann-Whitney U were used. *n*=4.

Figure 7: neutral sphingomyelinase controls p47phos expression.

siRNA against neutral sphingomyelinase (SMAse) prevents on p47phox expression induced by MetS MPs at 4 hours (A), but not at 24 hours (B). *P<0.05. For statistical analyses, one-way analysis of variance and Mann-Whitney U were used. *n*=4.

Figure 8: Schematic overview of effects of T lymphocytic

microparticles (MPs) (A) and MPs from metabolic syndrome patients (MetS MPs) (B) on endothelial cells. (A) MPs from apoptotic T cells act on Fas and LDL-receptors, then, via neutral SMase cascade induce cytosolic ROS production which activates ER stress. Through the interaction between ER and mitochondria, mitochondrial ROS are increased and contribute to decreased bioavailability of NO \cdot and the subsequent impairment of endothelium-dependent vasorelaxation. **(B)** Fas/FasL, but not LDL-receptor, participates in the response induced by MetS MPs. In addition, neutral SMase activation induces directly ER stress which, in turn, increases both cytosolic and mitochondrial ROS. All of these events lead to reduction of NO \cdot release and the subsequent impairment of endothelium-dependent vasorelaxation.

Figure 1

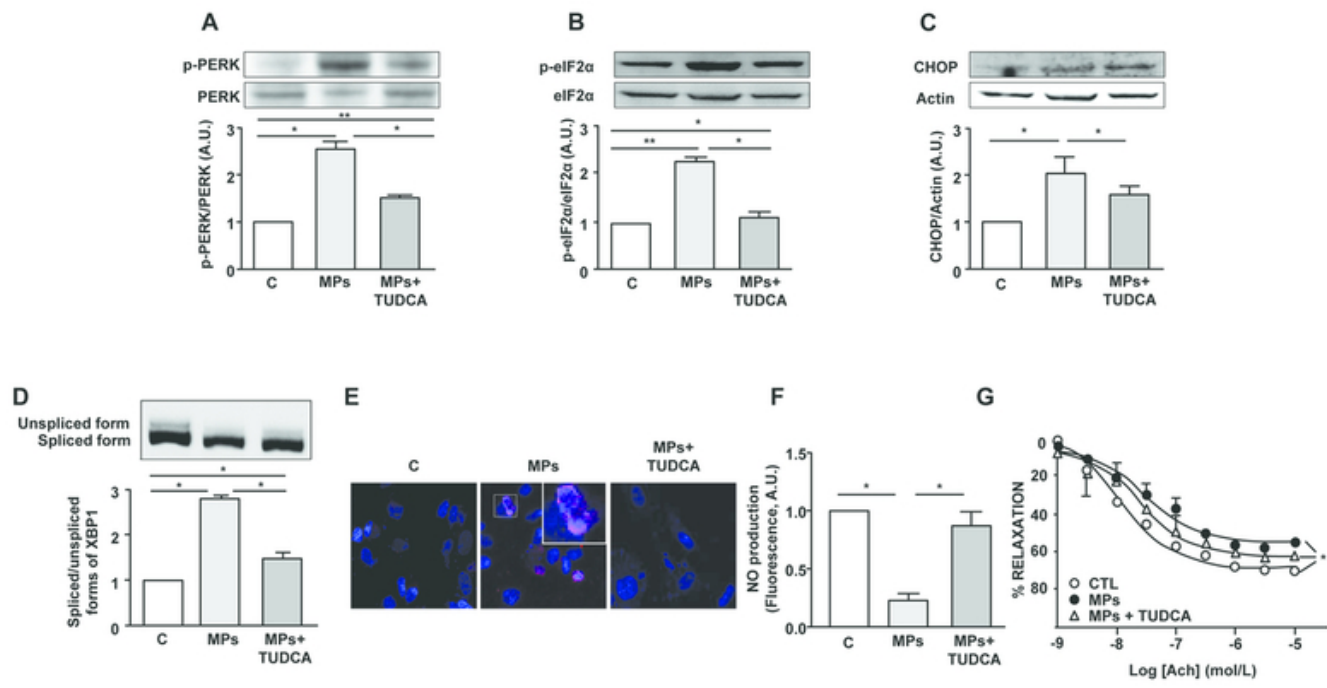


Figure 1

275x190mm (72 x 72 DPI)

Figure 2

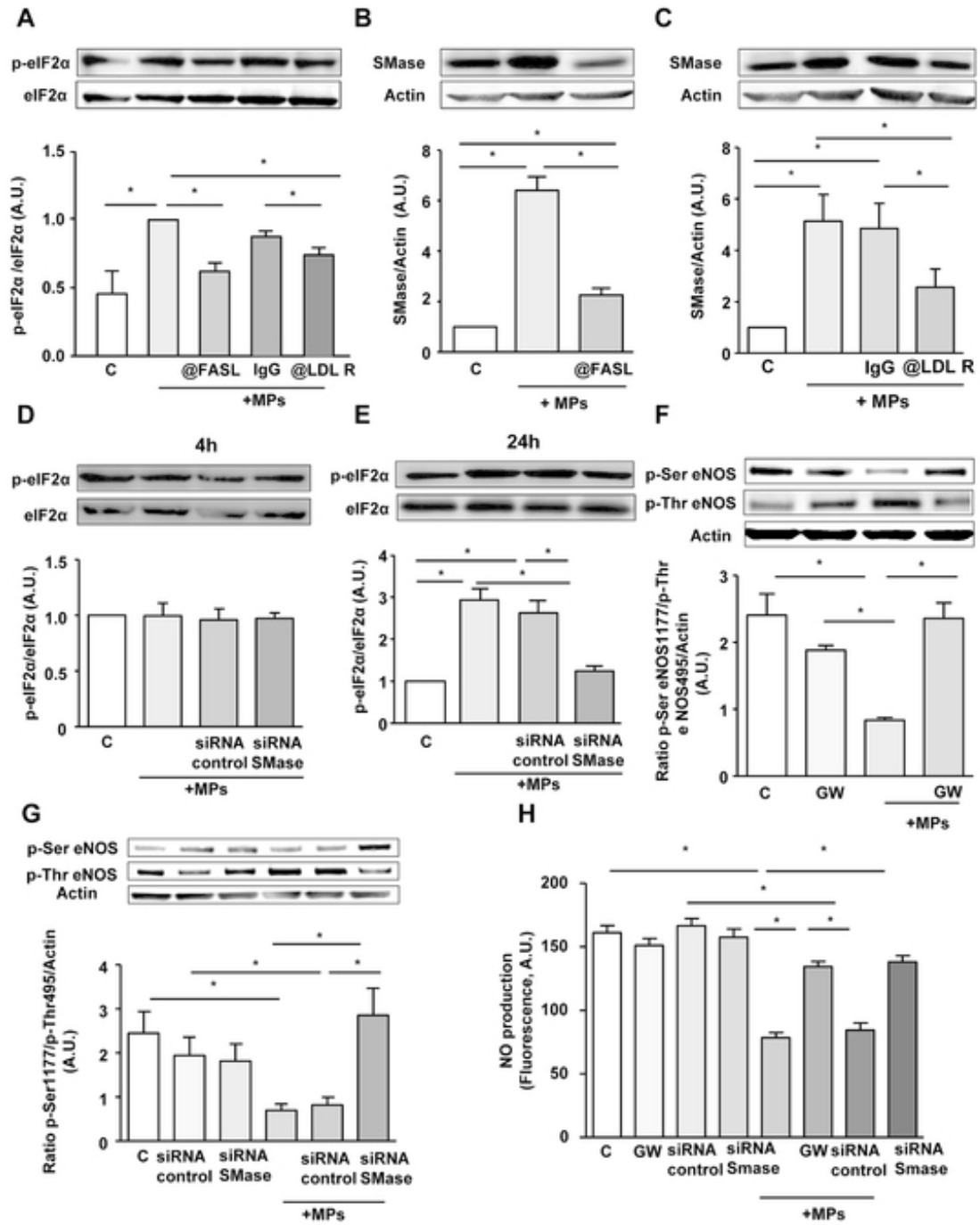


Figure 2

190x275mm (72 x 72 DPI)

Figure 3

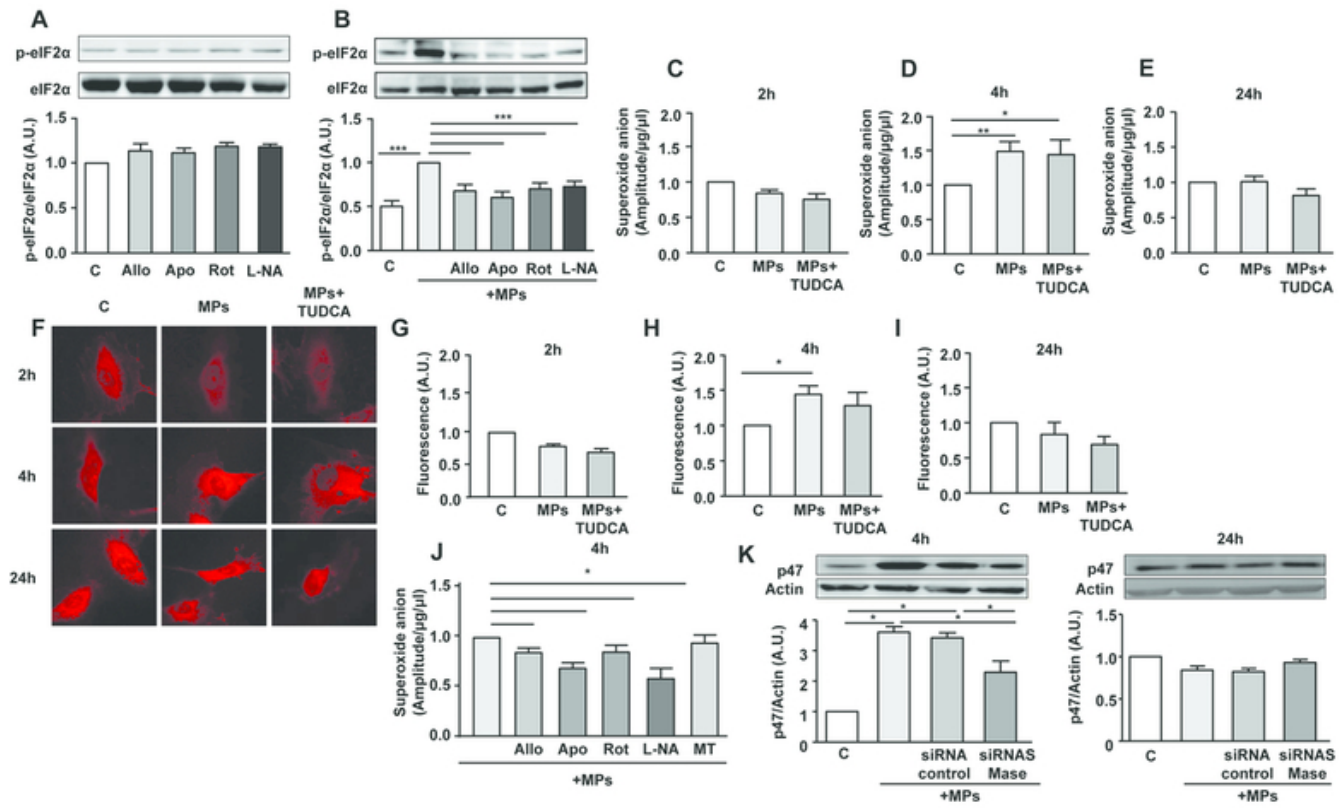


Figure 3

275x190mm (72 x 72 DPI)

Figure 4

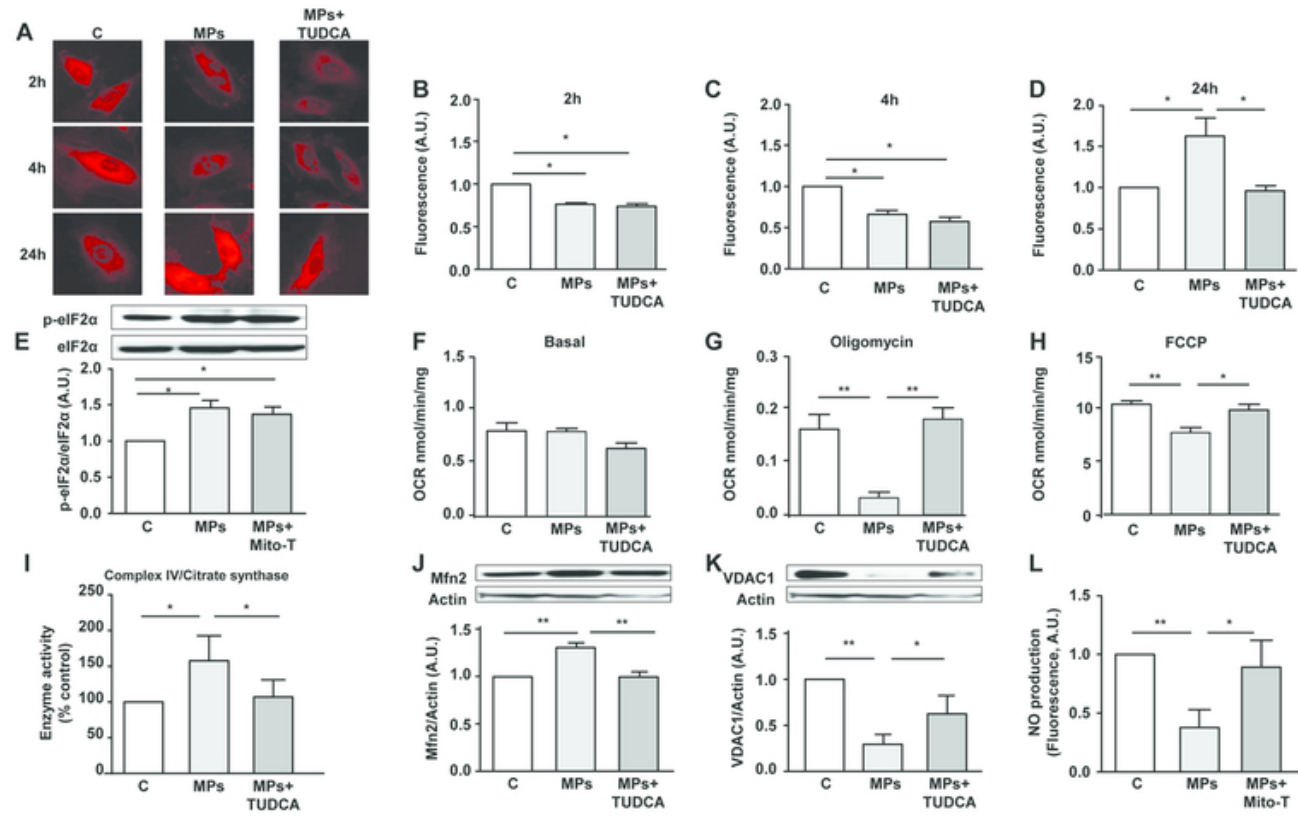


Figure 4

275x190mm (72 x 72 DPI)

Figure 5

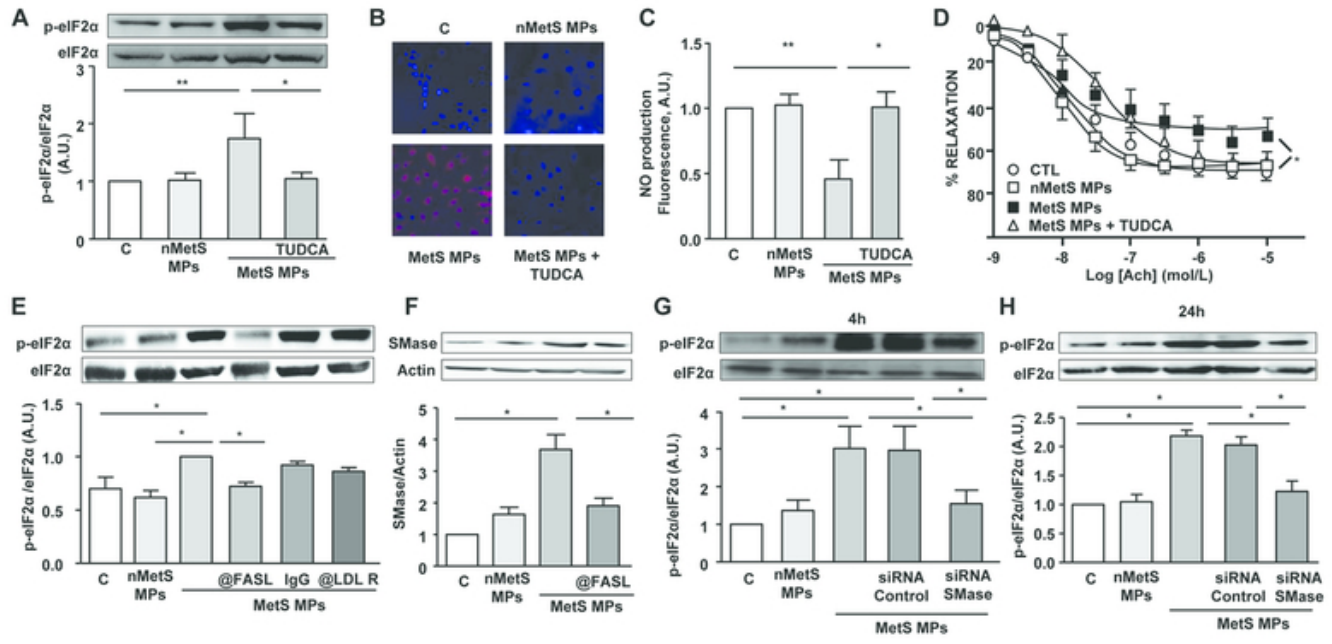


Figure 5

275x190mm (72 x 72 DPI)

Figure 6

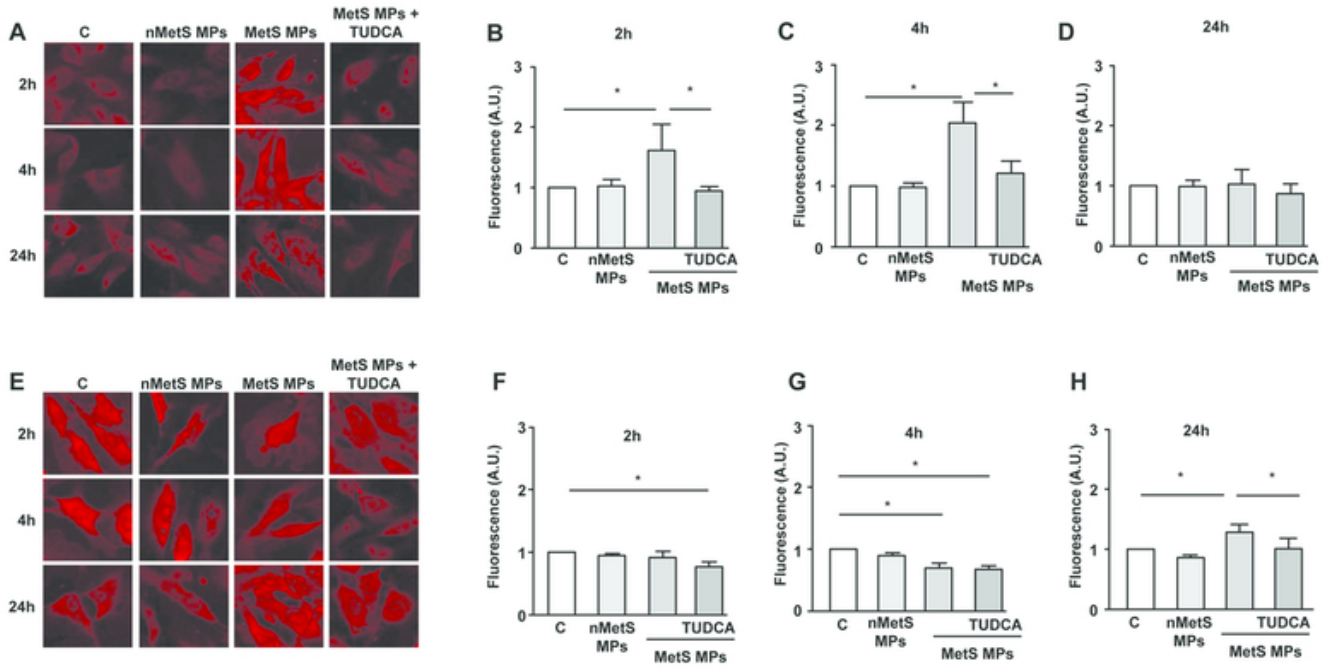


Figure 6

275x190mm (72 x 72 DPI)

Figure 7

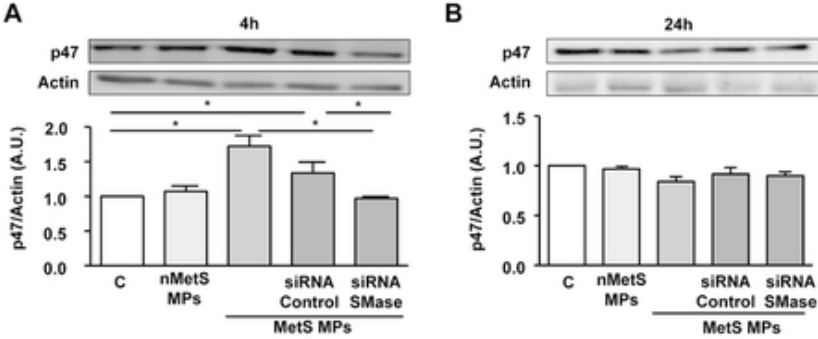


Figure 7

254x190mm (72 x 72 DPI)

Figure 7

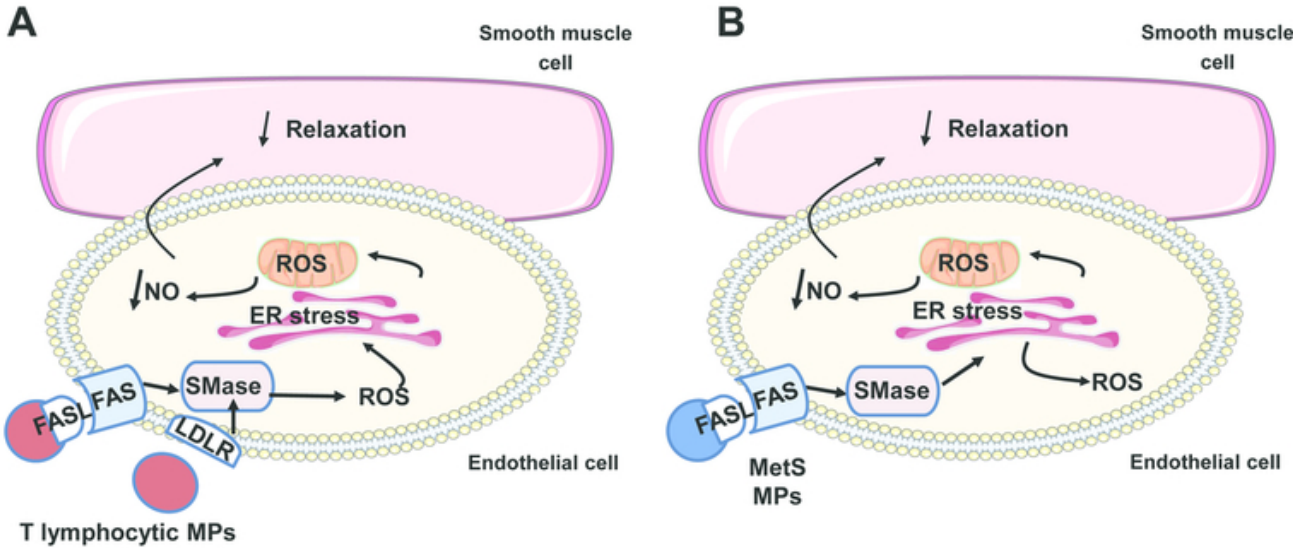


Figure 8

275x190mm (72 x 72 DPI)